Follicle-Stimulating Hormone Is an Autocrine Regulator of the Ovarian Cancer Metastatic Niche Through Notch Signaling

Sakshi Gera,[1] Sandeep Kumar S.,[2] Shalini N. Swamy,[2] Rahul Bhagat,[3] Annapurna Vadaparty,[3] Ramesh Gawari,[2] Ramray Bhat,[1] and Rajan R. Dighe[1]

[1]Department of Molecular Reproduction Development and Genetics, Indian Institute of Science, Bengaluru, 560012, India; [2]Department of Biochemistry, Kidwai Cancer Institute, Bengaluru, 560 029, India; and [3]Department of Biochemistry, Sri Shankara Cancer Hospital and Research Centre, Bengaluru, 560004, India

ORCiD numbers: 0000-0003-0266-855X (R. R. Dighe).

The association between the upregulated Notch and FSH signaling and ovarian cancer is well documented. However, their signaling has been investigated independently and only in the primary tumor tissues. The aim of this study was to investigate the interactive effects of FSH and Notch signaling on ovarian cancer proliferation, formation, and maintenance of disseminated ovarian cancer cells. The roles of Notch and FSH in ovarian cancer pathogenesis were investigated with ovarian cancer cell lines and specific antibodies against Notch and FSH receptor (FSHR). FSH upregulated Notch signaling and proliferation in ovarian cancer cells. High levels of FSH were detected in the ascites of patients with serous ovarian adenocarcinoma. Spheroids from the patients' ascites, as well as the spheroids from ovarian cancer cell lines under low attachment culture conditions, expressed $FSH\beta$ subunit mRNA and secreted the hormone into the medium. In contrast, primary ovarian tumor tissues and cell line monolayers expressed very low levels of $FSH\beta$. Ovarian cancer cell spheroids also exhibited higher expression of FSH receptor and Notch downstream genes than their monolayer counterparts. A combination of FSHR and Notch antagonistic antibodies significantly inhibited spheroid formation and cell proliferation *in vitro*. This study demonstrates that spheroids in ascites express and secrete FSH, which regulates cancer cell proliferation and spheroidogenesis through Notch signaling, suggesting that FSH is an autocrine regulator of cancer metastasis. Furthermore, Notch and FSHR are potential immunotherapeutic targets for ovarian cancer treatment.

Ovarian cancer is the leading cause of death among the gynecological malignancies [1]. One of the many risk factors recognized for ovarian cancer is excessive exposure of the normal ovarian surface epithelium to gonadotropins, FSH and LH, during menopause, ovulation, or infertility therapy [2–4]. The gonadotropins are heterodimeric glycoproteins, comprising a common α subunit associated noncovalently with the hormone-specific β subunit, secreted by the anterior pituitary, and are essential for follicular development in the ovary [5]. In addition, FSH stimulates growth of ovarian cancer cells [6, 7] while inhibiting apoptosis [8, 9].

Notch signaling plays role in a wide spectrum of cell fate decisions. There are four Notch receptors (Notch1 - Notch4) and four ligands (Jagged1 and 2, Delta1 and 4) known in mammals. A direct link between aberrant Notch signaling and ovarian cancer progression has been previously reported [10].

With progression of ovarian cancer, cells detach from the primary tumor as single cells or cellular aggregates called spheroids, which either remain in the ascites and contribute to disease recurrence or attach to the peritoneum for the development of secondary tumors [11]. Spheroids have been shown to be less susceptible to chemotherapy than single cells, and disruption of spheroids resensitizes ovarian tumor cells to chemotherapy with platinum-based drugs [12, 13].

In this study, the link between FSH and Notch pathways has been investigated in detail in three different ovarian cancer cell lines. We demonstrate that FSH upregulates Notch signaling in these cell lines. Furthermore, we demonstrate higher levels of FSH in the ascites of patients with ovarian cancer and trace the origin of this FSH to spheroids obtained from patients.

1. Materials and Methods

A. Ovarian Cancer Cell Lines

Ovarian cancer cell lines OVCAR-3, SKOV-3, and OVCAR-4 were authenticated by short tandem repeat analysis. OVCAR-3 cells were maintained in RPMI-1640 medium (Sigma, St. Louis, MO) supplemented with 15% fetal bovine serum (FBS) (Gibco, Paisley, United Kingdom). SKOV-3 cells were maintained in McCoy's medium (Sigma), and OVCAR-4 cells were maintained in DMEM (Sigma) supplemented with 10% FBS. IOSE-364, a kind gift from Dr. Pritha Ray (Advanced Centre for Treatment, Research and Education in Cancer, Navi Mumbai), was also cultured in DMEM supplemented with 10% FBS. All media were supplemented with penicillin and streptomycin (Gibco).

B. Hormone and Antibodies

Iodination grade-purified hormones and cAMP antiserum [14] were obtained from the National Hormone and Pituitary Program. Polyclonal antibodies against FSH receptor (FSHR) extracellular domain (RF5 a/s) [15, 16] and Notch3 receptor negative regulatory region (NRR a/s) [17, 18] were raised in rabbits according to a well-established immunization protocol [19]. Single-chain variable fragments (ScFv) against Notch3 NRR were isolated from the yeast display library according to a standardized protocol [20]. The interesting ScFv clone (ScFv42) [21] was expressed in *E. coli Bl21* and purified by 6XHis tag affinity chromatography.

C. FSHR Binding Assay

Binding of FSH to the receptors present on the ovarian cancer cell lines was analyzed by radioreceptor assay. FSH was radio-iodinated with the iodogen method [22]. The specific binding of ^{125}I-FSH to membrane preparations from the ovarian cancer cell lines was demonstrated as described earlier [23].

D. In Vitro *cAMP Measurement*

Approximately 1×10^5 OVCAR-3 cells per well were plated in a 48-well plate and 24 hours later were incubated with fresh medium containing 1 mM phosphodiesterase inhibitor 3-isobutyl-1-methylxanthine (IBMX) for 30 minutes at 37°C in a CO_2 incubator (100 μL) and then incubated with varying concentrations of FSH for 15 minutes (100 μL), after which the cells were lysed in 200 μL of 0.2 N HCl, and total cAMP produced was determined by RIA as described earlier [15].

E. Flow Cytometry–Based Detection of FSHR and Notch Receptors

Ovarian cancer cells were detached from the tissue culture flasks with 0.5 mM EDTA in Dulbecco's phosphate-buffered saline (DPBS) and resuspended in a medium containing 10% FBS. Approximately 1×10^5 cells were incubated with the primary antibody (Notch3 NRR a/s or RF5 a/s) at dilution of 1:500 for 1 hour at 4°C, followed by washing thrice with DPBS and resuspension in 100 μL of the medium with 10% FBS and 1:1000 dilution of anti-rabbit IgG fluorescein isothiocyanate (FITC; Invitrogen Camarilo, CA) for 45 minutes at 4°C. After incubation, the cells were washed and resuspended in DPBS and analyzed with the Becton Dickinson Accuri, and the median fluorescence values were analyzed.

F. Notch Signaling Assays

Notch signaling in the ovarian cancer cell lines was determined as described earlier [24]. Briefly, the ovarian cancer cell lines were seeded (5×10^4 cells per well) in 24-well plates and transfected with 790 ng of 12XCSL (CBF1/Su(H)/Lag-1) reporter plasmid and 10 ng of pGL3 basic or 800 ng of pGL3 control along with 1 ng of pRL-Tk with Lipofectamine 2000 (Invitrogen, Carlsbad, CA) according to the manufacturer's instructions. The 12XCSL reporter vector was a kind gift from Professor Urban Lendahl [25]. The vector contains the multimerized high-affinity CSL sites upstream of the luciferase reporter gene. The Notch intracellular domain after activation translocates to the nucleus and acts as a transcriptional regulator of CSL-dependent pathways and thus upregulates the expression of luciferase reporter in transfected cells. The transfected cells were incubated with increasing concentrations of FSH in presence or absence of RF5 a/s, Notch inhibitor N-[N-(3,5-difluorophenacetyl)-l-alanyl]-S-phenyl-glycine t-butyl ester (DAPT), 5 μM (Sigma) or ScFv42 (10 μg/mL), and the luciferase reporter activity was estimated with the Dual-Luciferase assay kit (Promega, Madison, WI) in the TD200 luminometer.

G. Ovarian Cancer Cell Line Proliferation

Proliferation of the ovarian cancer cell lines was determined with a 5-bromo-2′-deoxyuridine (BrdU) incorporation assay. Briefly, 5×10^3 cells were seeded per well in a 96-well plate and synchronized by incubation in medium without FBS overnight. Next day, the cells were treated with FSH or FSHR and Notch antagonists in the medium supplemented with FBS. The cells were labeled with BrdU for 12 hours, and its incorporation was determined according to the manufacturer's recommendation (Calbiochem, MilliporeSigma, Burlington, MA).

H. Expression Analysis by Real-Time PCR

Total RNA from ovarian tumors or spheroids obtained by peritoneal tap or from the ovarian cancer cell lines was isolated by the TRIzol-based method. Briefly, the cells were washed with DPBS and lysed in Trireagent (Sigma, Darmstadt, Germany). RNA was extracted according to the manufacturer's recommended protocol, and cDNA was synthesized from 1 μg of total RNA with the cDNA preparation kit (Thermo Scientific, Lithuania, Europe) and random primers. The transcript levels of the genes of interest were analyzed with SYBR Green in an Eppendorf RealPlex thermocycler and glyceraldehyde 3-phosphate dehydrogenase (GAPDH). The ΔΔCt method was used to calculate the fold difference in transcript levels of different genes. The absolute expression of FSH and FSHR in primary tumors and spheroids was interpolated from the dilution curve of the respective genes generated in the same experiment. The sequences of primers used in the analysis are listed in Table 1.

I. Estimation of FSH in Patients' Ascites

FSH levels in the ascites and sera of patients and the hormone secreted by the ovarian cancer cell lines were determined by RIA [15].

Table 1.   List of Real-Time Primers

Notch1	FP 5′ GTCAACGCCGTAGATGACC 3′
	RP 5′ TTGTTAGCCCCGTTCTTCAG 3′
Notch2	FP 5′ ATGACTGCCCTAACCACAGG 3′
	RP 5′ TGCAGTCATCTCCACTCCAG 3′
Notch3	FP 5′ GGGAAAAAGGCAATAGGC 3′
	RP 5′ GGAGGGAGAAGCCAAGTC 3′
Notch4	FP 5′ AACTCCTCCCCAGGAATCTG 3′
	RP 5′ CCTCCATCCAGCAGAGGTT 3′
Jag1	FP 5′ TCACGGGAAGTGCAAGAGTC 3′
	RP 5′ GTTTCAACAGTAGGCCCCCTC 3′
Jag2	FP 5′ CCCACCTGTGCCCTTGACA 3′
	RP 5′ GGCTTCCCCTTCACAGTCGTTGA 3′
Dll1	FP 5′ GCAGCTCTTCACCCTGTTCT 3′
	RP 5′ GGTGCAGGAGAAGTCGTTCA 3′
Dll4	FP 5′ ACGAATGCATCCCCCACAAT 3′
	RP 5′ GACAGGTGCAGGTGTAGCTT 3′
Hes1	FP 5′ TTCCCTCCGGACTCTAAACA 3′
	RP 5′ CAAACATCTTTGGCATCACA 3′
Hes5	FP 5′ GCCGTTTTAGGACAATCAGG 3′
	RP 5′ GAGTTCGGCCTTCACAAAAG 3′
Heyl	FP 5′ AGAATCCCTAGTGGGGCTGT 3′
	RP 5′ GGCTTGGGGATAGAAACACA 3′
FSHR	FP 5′ AACACCCATCCAAGGAATGG 3′
	RP 5′ GGGCTAAATGACTTAGAGGGACAA 3′
FSHβ	FP 5′ ATACAAGGAATCTGCATGGTGAG 3′
	RP 5′ TGGTGTGCTGGCTACTGCTAC 3′
FSHα	FP 5′ TCCCACTCCACTAAGGTCCAA 3′
	RP 5′ CCCCATTACTGTGACCCTGTT 3′
GAPDH	FP 5′ GAGAAGGCTGGGGCTCATTT 3′
	RP 5′ AGTGATGGCATGGACTGTGG 3′
RPL35	FP 5′ TCTAAGATCCGAGTCGTCCG 3′
	RP 5′ GCATGGCACGTGTCTTCTTA 3′

J. Spheroid Formation by Ovarian Cancer Cell Lines

Cellular aggregates of the ovarian cancer cell lines were developed by culturing the cells under low-attachment conditions. Briefly, the cells (~10^4 per well) were seeded in 96-well low-attachment plates and allowed to form aggregates for 24 to 96 hours. The aggregates were treated with RF5 a/s or ScFv42 at different time points. At regular intervals, images of the aggregates were captured with a Zeiss microscope at ×60 magnification. The effects of different treatments on cellular aggregation or disaggregation were determined by analyzing the area of aggregates in a script developed in MATLAB R15a (100 pixels in the image was equivalent to 150 μM), with the ellipticity held constant at 0.1.

K. Statistical Analyses

Statistical analyses were performed in Graphpad Prism 5.0 software. A P value <0.05 was considered statistically significant. Each experiment was repeated three times.

2. Results

## A. FSH and Notch Signaling in the Ovarian Cancer Cell Lines

The presence of functional FSHR and Notch receptors in the ovarian cancer cell lines (OVCAR-3, SKOV-3, and OVCAR-4) was demonstrated through different approaches. The presence of FSHR in these cells was demonstrated by determining specific binding of ^{125}I-FSH to the ovarian cancer cell membranes. The membrane preparations were incubated with

^{125}I-FSH in presence of increasing concentrations of unlabeled FSH, and the binding data obtained were converted into Scatchard plots. As shown in Fig. 1A, the dissociation constants of OVCAR-3 and SKOV-3 were 1.7×10^{-9} M and 1.9×10^{-9} M, respectively, whereas that of OVCAR-4 was 2.8×10^{-9} M. The B_{max} for the receptor was highest in the OVCAR-3 cells (Fig. 1A).

The presence of FSHR on ovarian cancer cells was also confirmed by flow cytometry with the antiserum raised against FSHR (RF5 a/s) [15]. The cells were incubated with RF5 a/s, and its binding was determined with anti-rabbit IgG-FITC. As shown in Fig. 2A, all three ovarian cancer cell lines exhibited binding of the a/s, indicating the presence of FSHR on their surfaces, with OVCAR-3 cells displaying the highest antibody binding, which agrees with the Scatchard analysis. Furthermore, six-fold higher expression of FSHR was observed at the mRNA level in OVCAR-3 cells compared with normal ovarian epithelial cell line IOSE 364.
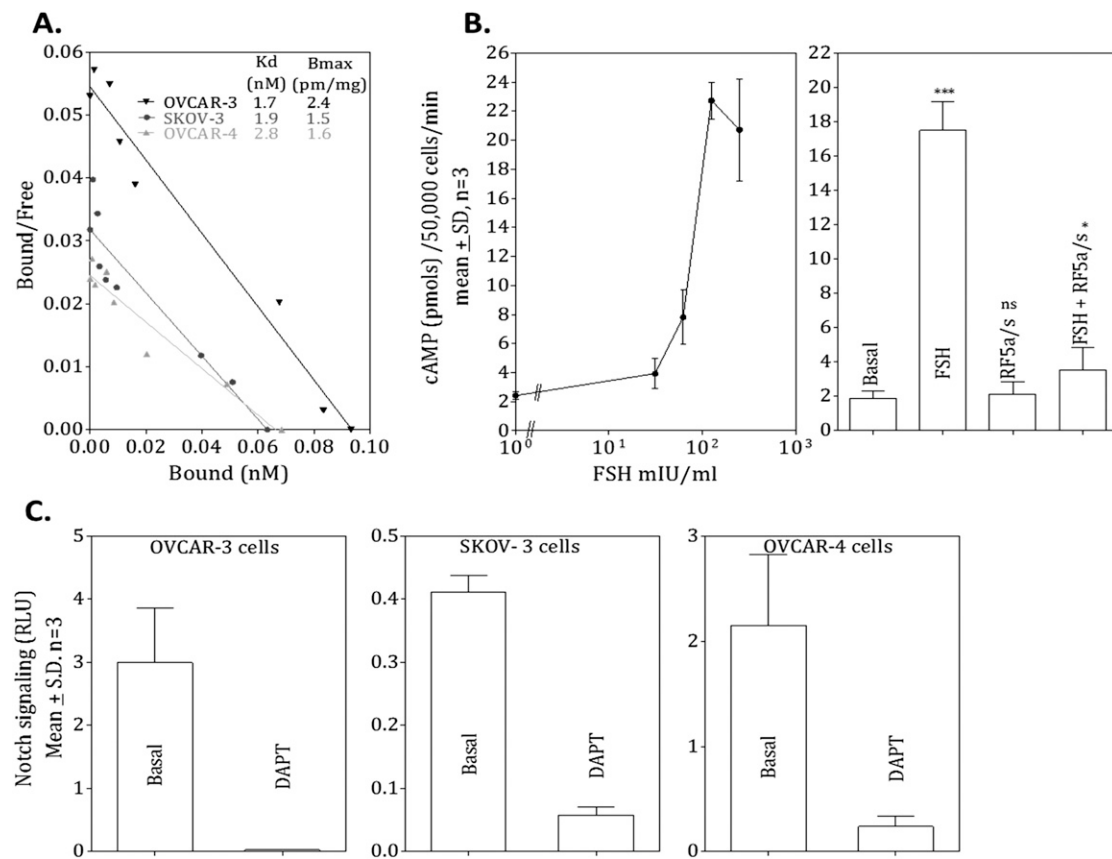
Figure 1. Characterization of FSH signaling in ovarian cancer cell lines. (A) The presence of FSHR on ovarian cancer cell lines OVCAR-3, SKOV-3, and OVCAR-4 was investigated by determining the binding of ^{125}I-FSH to their membranes (10 μg each) in the presence of increasing concentrations of cold FSH. The binding data were converted to a Scatchard plot, and the inset table shows the K_d and B_{max} of hormone in the three cell lines. (B) The activity of FSHR was investigated by analyzing the levels of cAMP in the presence of hormone by RIA. OVCAR-3 cells were incubated with increasing concentrations of FSH or with 100 mIU/mL FSH in the presence and absence of 5 μg/mL of RF5 a/s, and cAMP levels were determined. Significance was calculated by comparing the treated with basal values *via* nonparametric unpaired *t* test. (C) Ovarian cancer cells were transfected with 12XCSL luciferase reporter plasmid and incubated with 5 μM DAPT to determine Notch signaling activity. Reporter activity was analyzed after 24 h of incubation by dual luciferase assay. ns, $P > 0.05$; *$P \leq 0.05$; ***$P \leq 0.001$. Error bars represent mean ± SD, and n is the number of repeats. RLU, relative luciferase unit.
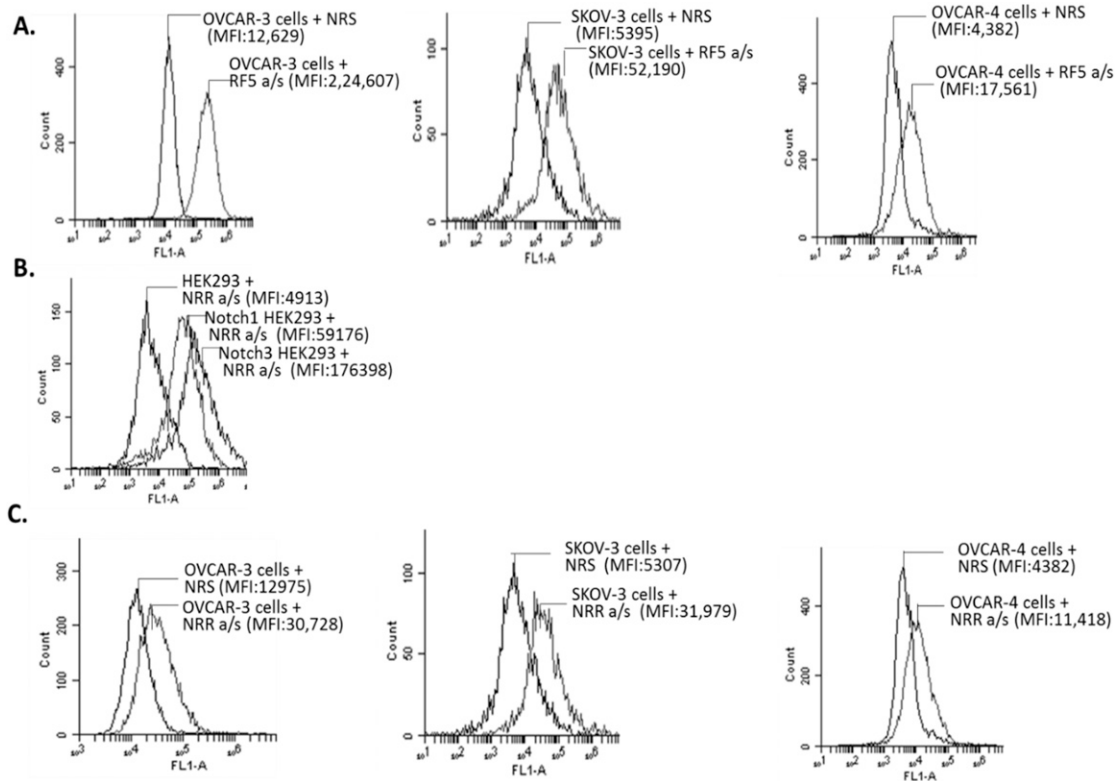
Figure 2. FSHR on ovarian cancer cell lines. (A) The presence of FSHR on ovarian cancer cell lines OVCAR-3, SKOV-3, and OVCAR-4 was analyzed by flow cytometry. The ovarian cancer cell lines were incubated with RF5 a/s (1:500 dilution) or normal rabbit a/s (NRS) and analyzed for binding with FITC-conjugated anti-rabbit secondary antibody. The histograms represent three independent experiments. (B) HEK293 cells and Notch1- and Notch3-overexpressing HEK293 cells were incubated with Notch3 NRR a/s (1:500 dilution) followed by anti-rabbit FITC, and binding was analyzed by flow cytometry. (C) The presence of Notch receptor on ovarian cancer cell lines OVCAR-3, SKOV-3, and OVCAR-4 was analyzed by flow cytometry. The ovarian cancer cell lines were incubated with Notch3 NRR a/s (1:500 dilution) or normal rabbit a/s (NRS) and analyzed for binding by anti-rabbit secondary antibody conjugated with FITC. The histograms represent three independent experiments. MFI, median fluorescent intensity.

The functional nature of FSHR was further confirmed by determining the response of OVCAR-3 cells to FSH *in vitro*. The cells were incubated with increasing concentrations of FSH for 15 minutes at 37°C, and cAMP formed was determined by RIA. As shown in Fig. 1B, FSH produced a dose-dependent increase in cAMP. In the next experiment, OVCAR-3 cells were incubated with FSH in the presence and absence of RF5 a/s, and cAMP produced was determined. As shown in Fig. 1B, response to the hormone was significantly inhibited in the presence of RF5 a/s, indicating the antagonistic nature of the a/s [15].

The presence of Notch receptors on the ovarian cancer cell lines was demonstrated by flow cytometry with the antiserum raised against the NRR of Notch3, which has full cross-reactivity with Notch1 (Fig. 2B). As shown in Fig. 2C, all three ovarian cancer cell lines exhibited binding of the NRR a/s, indicating the presence of Notch receptors on their cell surface. Notch signaling in OVCAR-3 cells, as determined by 12XCSL reporter, was stimulated by Dll4 (see below, Fig. 3C) and inhibited by DAPT (Fig. 1C).

B. Effect of FSH on Notch Signaling in the Ovarian Cancer Cell Lines
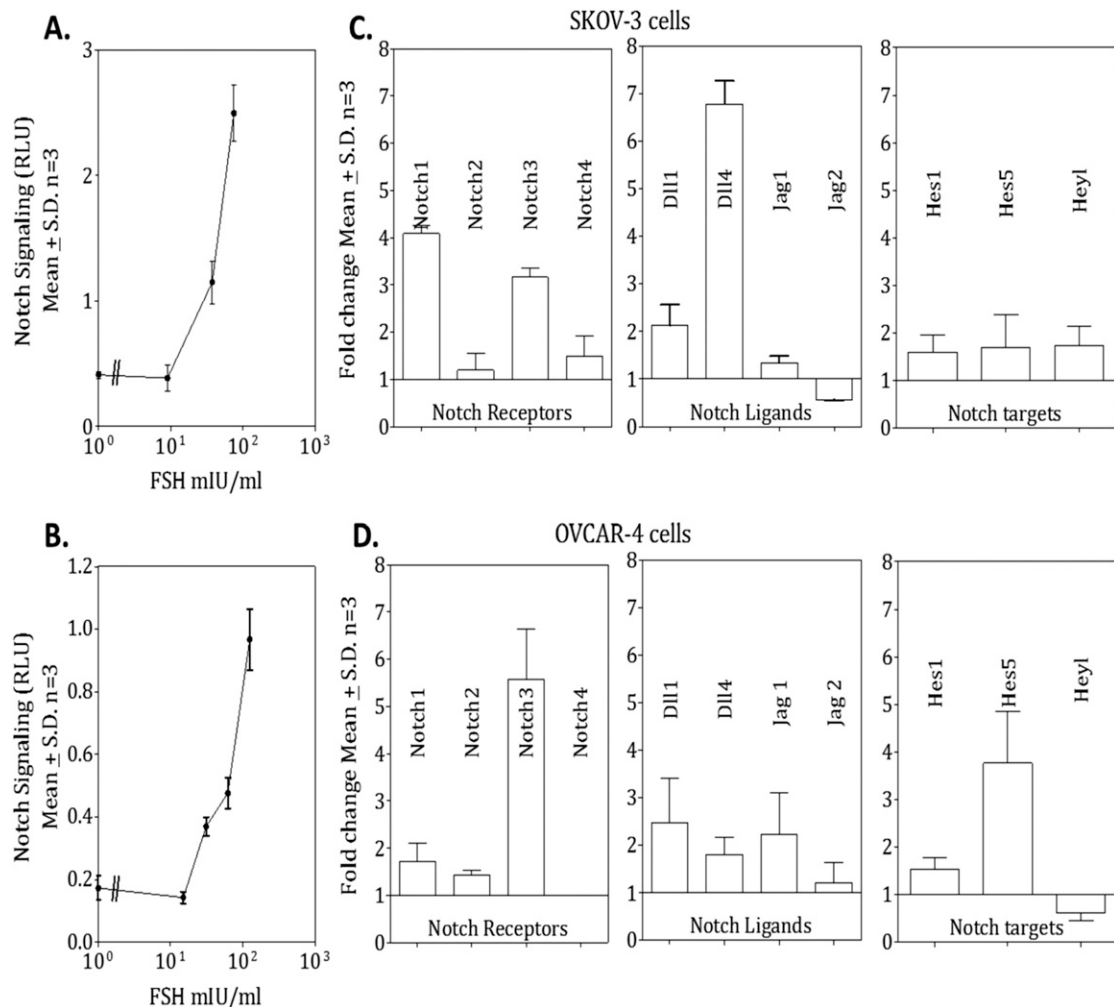
Possible effects of FSH on Notch signaling in the ovarian cancer cell lines were investigated by incubating the cell lines with increasing concentrations of FSH for 48 hours and
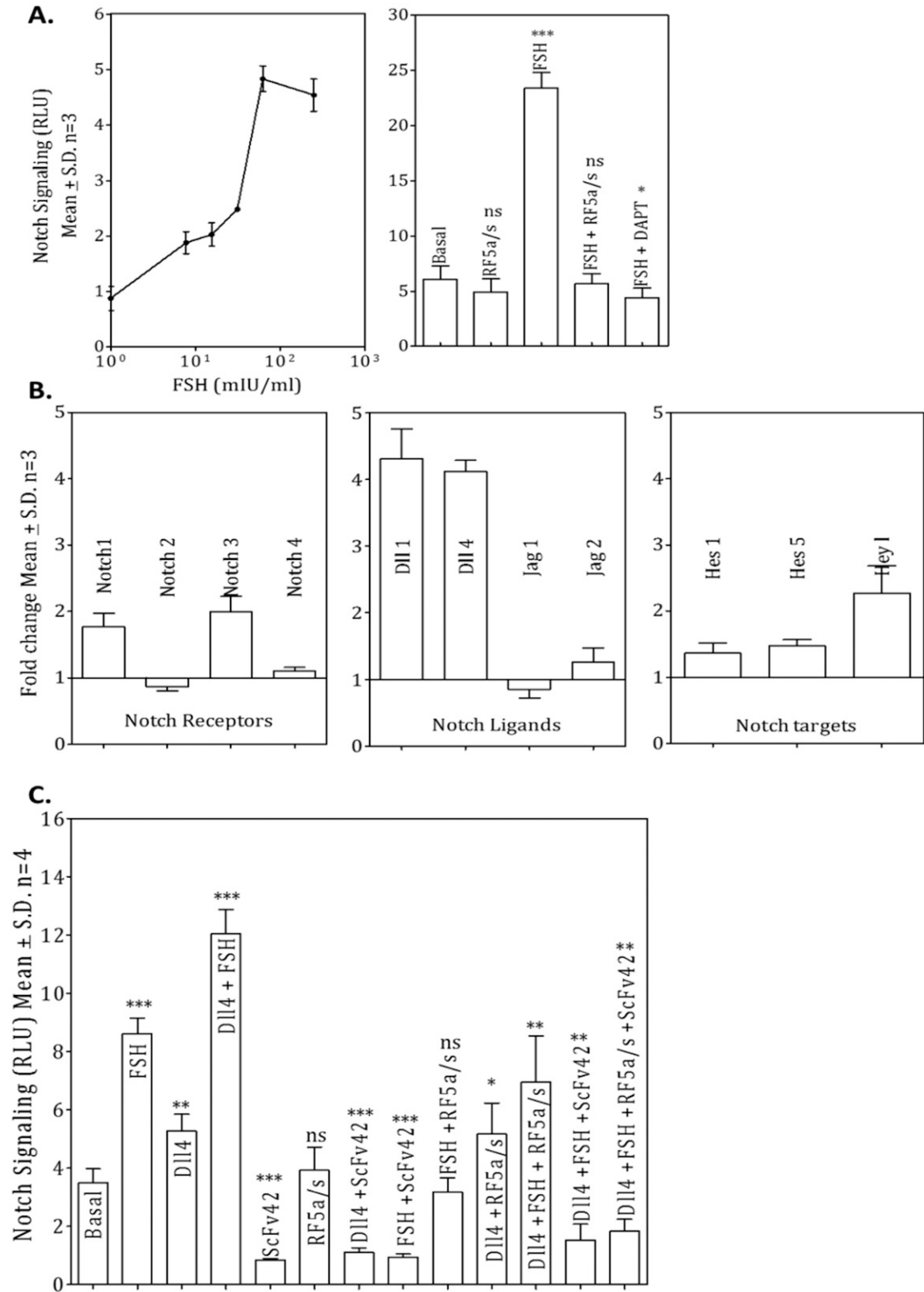
Figure 3. Effect of FSH on Notch signaling. (A) OVCAR-3 cells were transfected with 12XCSL luciferase reporter plasmid and incubated with increasing concentrations of FSH or 100 mIU/mL of FSH in the presence of 5 μg/mL FSHR antagonist RF5 a/s and 5 μM DAPT in different combinations for 48 hours. Reporter activity was measured by dual luciferase assay after 48 h of incubation. (B) OVCAR-3 cells were incubated with 100 mIU/mL of FSH for 48 hours, and RT-PCR was performed for indicated Notch receptors, ligands, and target

genes. The fold change in the expression of receptor and ligands was calculated with respect to cells cultured without hormone after normalizing with GAPDH expression. (C) OVCAR-3 cells transfected with 12XCSL luciferase reporter plasmid were cultured on precoated Dll4-Fc. 100 mIU/mL of FSH, 5 µg/mL FSHR antagonist RF5 a/s, and 10 µg/mL ScFv42 in different combinations were added to the cells for 48 h, and the effect on the Notch signaling was measured by dual luciferase assay. Significance is calculated by comparison of treated and basal values *via* nonparametric unpaired *t* test. ns, $P > 0.05$; *$P \leq 0.05$; **$P \leq 0.01$; ***$P \leq 0.001$ compared with basal values. Error bars represent mean ± SD, and n is the number of repeats. RLU, relative luciferase unit.

determining Notch signaling in cells expressing 12XCSL luciferase reporter. As shown in Fig. 3A, in OVCAR-3 cells there was an FSH dose-dependent increase in luciferase activity, indicating increased Notch signaling, which was further confirmed by increases in the transcript levels of Notch target genes *Hes1*, *Hes5*, and *Heyl* (Fig. 3B). Similar results were obtained for SKOV-3 and OVCAR-4 cells (Fig. 4A and 4B). The stimulatory effect of FSH on Notch signaling

Figure 4. Effect of FSH on Notch signaling. (A) SKOV-3 and (B) OVCAR-4 cells were transfected with 12XCSL luciferase reporter plasmid and incubated with increasing concentrations of FSH. The effect on the Notch signaling was measured by dual luciferase assay after 48 h. (C) SKOV-3 and (D) OVCAR-4 cells were incubated with 100 mIU/mL of FSH for 48 h, and RT-PCR was performed for indicated Notch receptors, ligands, and target genes. The fold change in the transcript levels of Notch genes was calculated with respect to the levels in cells cultured without hormone after normalizing with GAPDH expression. Error bars represent mean ± SD, and n is the number of repeats. RLU, relative luciferase unit.

was completely inhibited by the RF5 a/s, which by itself had no effect on Notch signaling. The hormone-stimulated Notch signaling was also inhibited by DAPT (Fig. 3A).

FSH upregulated expression of *Notch1* and *Notch3*, as well as Notch ligands *Dll1* and *Dll4* in OVCAR-3 cells, as determined by RT-PCR (Fig. 3B). In addition, an increase in Notch receptors and Dll4 was demonstrated by flow cytometry (Fig. 5). In the OVCAR-4 cell line, upregulation was observed predominantly for Notch3 and the three ligands, *Jag1*, *Dll1*, and *Dll4* (Fig. 4B). Thus, increased Notch signaling in the ovarian cancer cell lines in response to FSH was a result of increased expression of both Notch receptors and ligands.

Dll4 present on the surface of stromal cells in the ovarian cancer microenvironment is involved in progression of ovarian tumors [26], and as described above, FSH upregulates Dll4 expression. Therefore, the effect of exogenous Dll4 [24] together with FSH on Notch signaling was determined. The OVCAR-3 cells were incubated with FSH (100 mIU/mL) and the immobilized Dll4, individually and in combination, and Notch signaling was determined. As shown in Fig. 3C, both ligands stimulated Notch signaling in an additive manner. The effects of RF5 a/s and Notch inhibitory ScFv42 on Notch signaling were investigated in the same experiment. ScFv42 is a Notch3 NRR-specific ScFv and can inhibit basal and FSH-stimulated Notch signaling in a dose-dependent manner (Fig. 6). As shown in Fig. 3C, RF5 a/s inhibited FSH-stimulated Notch signaling, whereas ScFv42 inhibited basal, Dll4-, FSH-, and FSH+ Dll4-stimulated Notch signaling. A combination of RF5 a/s and ScFv42 inhibited Notch signaling to the same extent as ScFv42 alone.

C. Effects of FSH and Notch Ligand on the Proliferation of Ovarian Cancer Cell Lines

The role of Notch signaling in the proliferation of ovarian cancer cell lines is well documented, and as shown above, FSH upregulated Notch signaling in the ovarian cancer cell lines.
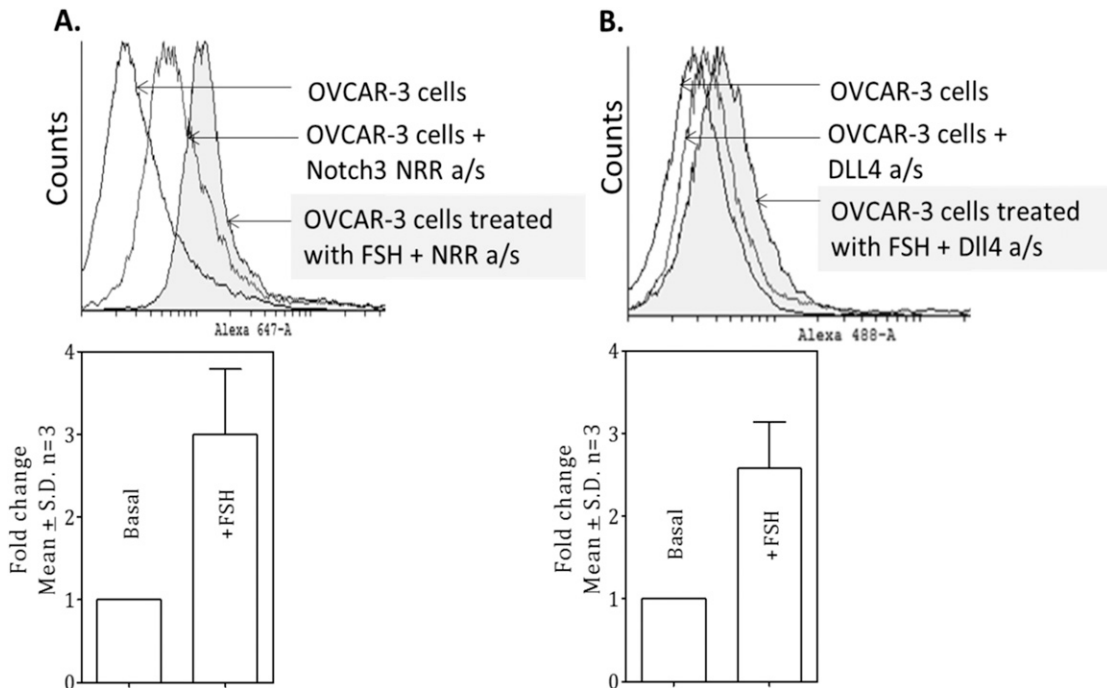
Figure 5. Effect of FSH on Notch receptors and ligands. OVCAR-3 cells were harvested with EDTA after incubation with 100 mIU/mL of FSH for 48 hours and labeled with (A) Notch3 NRR a/s and (B) Dll4 antibody for analysis by flow cytometry. The antibody bound was determined by anti-rabbit Alexa 647 and anti-mouse Alexa 488, respectively. Binding of a/s was analyzed by comparing the median fluorescent intensity in the presence and absence of hormone. The histograms represent three independent experiments. Quantitative analysis of the same is represented in the bar graphs. Significance is calculated by comparison of treated and basal values *via* nonparametric unpaired *t* test. Error bars represent mean ± SD, and n is the number of repeats.
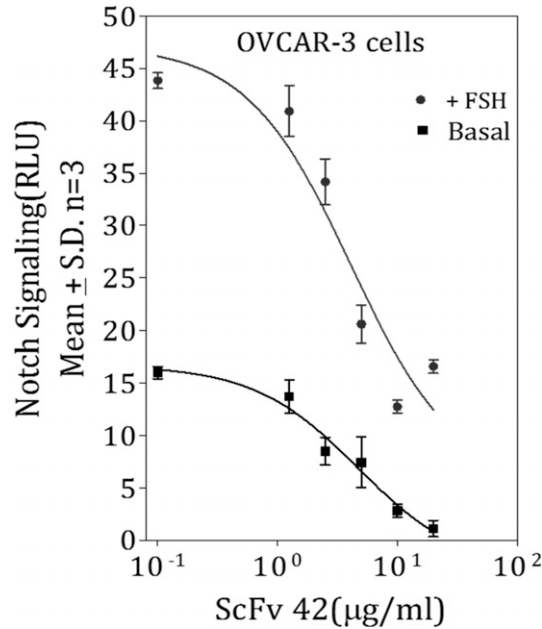
Figure 6. Effect of anti-Notch3 ScFv on Notch signaling. OVCAR-3 cells were transfected with luciferase plasmid and incubated with increasing concentrations of ScFv42 (Notch3 NRR antagonist) in the presence or absence of 100 mIU/mL FSH. Reporter activity was measured by dual luciferase assay after 48 h of incubation. n is the number of repeats. RLU, relative luciferase unit.

Therefore, the effect of FSH on the proliferation of OVCAR-3 cells was determined. OVCAR-3 cells were incubated with increasing concentrations of hormone for 48 hours, and BrdU incorporation was analyzed. As shown in Fig. 7A, FSH stimulated OVCAR-3 cell proliferation in a dose-dependent manner.

Next, the effects of FSH and Notch ligand, individually and in combination, on proliferation of the OVCAR-3 cell line were examined. As shown in Fig. 7B, both ligands stimulated cell proliferation in an additive manner. This increase in proliferation was inhibited by RF5 a/s, as well as ScFv42. Furthermore, the FSH- and Dll4-stimulated proliferation were inhibited by both RF5 a/s and the Notch3 NRR-specific ScFv, even below the basal level.

D. FSH Levels in Patients' Ovarian Tumors, Sera, and Ascites

To understand the role of FSH and Notch signaling in ovarian cancer progression, FSH levels in the ascites of patients with cancer were estimated. Ascites samples were obtained by peritoneal tap from 26 patients with ovarian cancer, serum samples were obtained from seven patients, and FSH levels were determined by RIA. FSH was detected in the ascites of all patients, with levels ranging from 15 mIU/mL to 208 mIU/mL. The serum could be the possible source of FSH in the ascites. Average serum FSH levels in postmenopausal Indian women (age 54 ± 8 years) were 62 ± 30 mIU/mL, and those in premenopausal women were 25.8 ± 10 mIU/mL [27, 28]. As shown in Table 2, ascitic FSH levels in 12 patients (patients 2, 3, 6, 10, 11, 12, 13, 14, 17, 18, 23, and 25) were >62 mIU/mL, whereas the seven patients who had low FSH in their ascites either did not have malignant cells detected in their ascites (patients 1, 8, 9, and 15) or were undergoing chemotherapy (patients 20, 21, and 24). Of the seven patients whose serum samples were available for analysis, three (patients 23, 25, and 26) showed high FSH levels in both serum and ascitic fluid (>100 mIU/mL). However, in the remaining four patients, there was no correlation between serum and ascitic FSH levels.

To identify the source of hormone in the ascites, primary ovarian tumor tissues from five patients with ovarian cancer (patients 27 to 31) were obtained. The total RNA was isolated
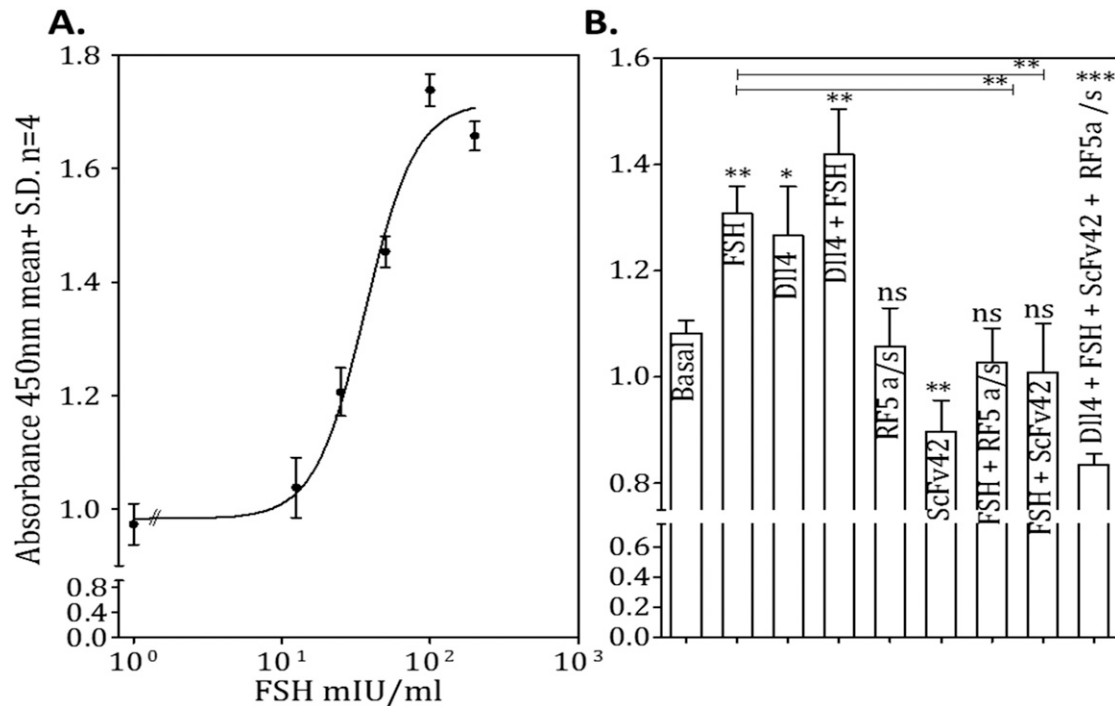
Figure 7. Effect of FSH on proliferation of ovarian cancer cells. (A) OVCAR-3 cells were synchronized by culturing in serum-free medium overnight and incubated with increasing FSH concentrations. The proliferation rate was investigated by analyzing the BrdU incorporation in the cells after 48 h. (B) OVCAR-3 cells [synchronized as in (A)] were cultured on precoated Dll4-Fc and incubated with 100 mIU/mL FSH, 5 μg/mL FSHR antagonist RF5 a/s, or 10 μg/mL ScFv42, in different combinations, for 48 h. Proliferation rate was investigated by BrdU incorporation, and significance was calculated by unpaired t test compared with the basal levels. ns, $P > 0.05$; *$P \leq 0.05$; **$P \leq 0.01$; ***$P \leq 0.001$ compared with basal values. n is the number of repeats. Error bars represent mean ± SD.

and subjected to RT-PCR analysis for *FSHα*, *FSHβ* and *FSHR* transcripts for the absolute quantification of RNA levels. The expression was quantified based on a dilution curve of known DNA concentrations for each gene. In addition, as a comparative positive control, human pituitary tissue was included for the expression of genes encoding *FSHα*, *FSHβ* and *FSHR*. As shown in the Fig. 8, patients' tumor samples exhibited lower expression of *FSHα* and *FSHβ* suggesting very low hormone message in the tumors, whereas the *FSHR* transcript levels were very high (patients 27, 28, 29, and 30). The possibility of FSH being expressed by the metastatic tumor epithelium represented by spheroids in ascitic fluid was next explored. Multicellular spheroids from the ascitic fluid of eight patients (patients 2, 3, 5, 10, 11, 13, 14, and 18) were isolated from cell mass, and as shown in the Fig. 8, the spheroids obtained from these patients exhibited high levels of *FSHβ* message, except those obtained from patient 5, who had recurrent disease (Table 2). The *FSHβ* transcript levels were consistent with the ascitic hormone levels. Interestingly, there was a significantly higher expression of *FSHR* in the spheroids of the patients with ovarian cancer (patients 2, 3, 10, 11, 13, 14, and 18) compared with those of patient 5 (Fig. 8).

E. Expression of FSH in Ovarian Cancer Cell Line Spheroids and Monolayers

To simulate the conditions of *in vivo* spheroid formation, the ovarian cancer cell lines were cultured under low-attachment conditions that facilitated the cells to aggregate and form compact spheroidal aggregates [29]. As shown in Fig. 9A, spheroid-like aggregates of OVCAR-3 cells were observed after 48 hours of culture. SKOV-3 and OVCAR-4 cells formed aggregates of different geometries under these conditions (Fig. 9B and 9C). Expression of FSH by the spheroids or aggregates was demonstrated by determining the hormone levels in the culture supernatants

Table 2. FSH in Patients' Ascites and Serum

Patient	Age (y)	Description	Ascitic FSH (mIU/mL)	Serum FSH (mIU/mL)
1	NA	Reactive mesothelial cells in a hemorrhagic background with a few inflammatory cells	22.2	NA
2	70	High-grade adenocarcinoma of ovary	71.04	NA
3	53	Metastatic adenocarcinoma of ovary	124.14	NA
4	58	High-grade serous papillary carcinoma, grade 3, stage 1B; recurrent disease	45.2	NA
5	50	High-grade serous adenocarcinoma, recurrent disease, stage IVB	38	NA
6	72	Serous adenocarcinoma	102.8	NA
7	49	Adenocarcinoma of ovary	36.6	NA
8	40	Shows normal squamous cells; no abnormal cells seen in cytology	34.2	NA
9	56	Peritoneal fluid shows reactive mesothelial cells; no malignant cells seen in ascites	13.5	NA
10	42	Serous adenocarcinoma	136.32	NA
11	50	Serous papillary adenocarcinoma	134.24	NA
12	48	NA	98.24	NA
13	45	Serous adenocarcinoma	90.96	NA
14	55	High-grade serous carcinoma; completed 6 CTs	96.32	NA
15	68	High-grade serous papillary carcinoma; patient undergoing CT at sample collection	15	NA
16	NA	NA	40.9	NA
17	NA	Serous adenocarcinoma, 5 cycles of CT completed	102.77	NA
18	54	High-grade serous papillary carcinoma	104.85	NA
19	53	High-grade serous papillary carcinoma	35.01	NA
20	55	Post-NACT, 3 cycles of CT	23.41	24.44
21	43	No residual disease	24	84.55
22	64	Serous adenocarcinoma, stage IIIC	40.83	0
23	58	Serous adenocarcinoma, grade 1	208.32	122.19
24	46	Post-NACT, stage III, serous adenocarcinoma	14.76	5.85
25	55	Serous adenocarcinoma	115.44	131.43
26	73	Post-NACT, 3 cycles of CTs, serous papillary adenocarcinoma	59.71	147.26
27	56	Metastatic adenocarcinoma of ovary	NA	NA
28	61	Mucinous low-grade ovarian carcinoma	NA	NA
29	46	Low-grade ovarian carcinoma	NA	NA
30	59	Ovarian malignant neoplasm	NA	NA
31	73	High-grade serous carcinoma; patient undergoing CT, post-NACT	NA	NA

Details of the patients from whom ascites, serum, and ovarian tumor samples were obtained. Levels of FSH in the ascites and serum obtained from the patients with ovarian cancer were determined by RIA in a single experiment. Abbreviations: CT, chemotherapy; NA, not available; NACT, neoadjuvant chemotherapy.

collected after different intervals and *FSHβ* transcript levels by RT-PCR. As shown in Fig. 9D and 9E, there was an increase in *FSHβ* transcripts under nonattachment conditions, with corresponding secretion of FSH by OVCAR-3 and SKOV-3 cells, whereas there was no increase in the *FSHβ* transcripts or in secreted FSH when the cells were grown as monolayer cells. OVCAR-4 cells did not show any increase in *FSHβ* transcripts or secreted hormone (Fig. 9F).

F. Effect of FSH and Notch Inhibitors on OVCAR-3 Spheroids

Formation of ovarian cancer cell line spheroids mimics the ovarian tumor metastatic condition, and these spheroids exhibit chemoresistance as they increase in size [30]. Higher chemoresistance has also been correlated with increased Notch signaling [31, 32]. Therefore, expression of Notch signaling genes was investigated in the spheroids. As shown in Fig. 10A and 10B, there was an increase in *Notch1*, *Notch3*, *Jag2* and *Dll4*, and the downstream genes
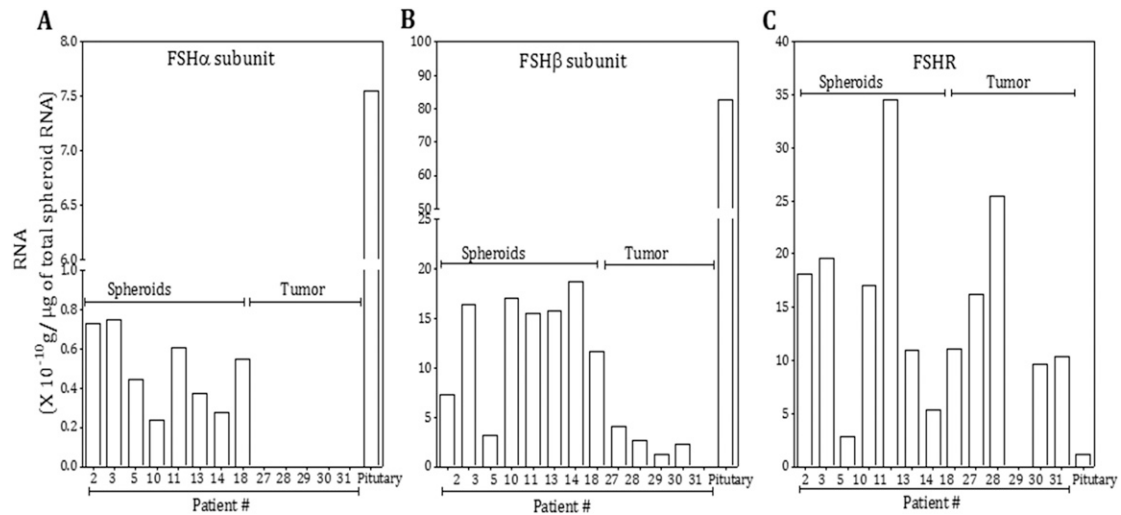
Figure 8. Expression of FSH and FSHR in primary tumor and spheroids obtained from patients with ovarian cancer. Total RNA was isolated from the primary tumors and spheroids obtained from the ascites of patients with ovarian cancer, and cDNA was prepared from 1 μg total RNA. Cycle threshold values of (A) FSHα subunit, (B) FSHβ subunit, and (C) FSHR were examined by RT-PCR, and RNA levels were interpolated from the dilution curves of the respective genes.

Hes1 and *Heyl*, as well as FSH receptor on spheroid formation. Thus, an upregulation of Notch signaling correlates with the increase in FSHβ and FSHR expression in ovarian cancer spheroids. Furthermore, as shown in Fig. 11A, the mean size of the aggregates formed was significantly less in the presence of RF5 a/s and ScFv42, and this effect was significantly increased in presence of both inhibitors.

In the next experiment, the effects of both these inhibitors on the preformed spheroids were investigated. OVCAR-3 cell aggregates were formed for 48 hours, and then RF5 a/s and ScFv42, individually or in combination, were added. As shown in Fig. 11B, there was a decrease in the mean aggregate size when both FSH and Notch signaling were inhibited.

3. Discussion

The etiology of ovarian carcinomatosis is not well understood. Both FSH and Notch have been shown to be involved in ovarian tumor angiogenesis, epithelial to mesenchymal transition, resistance to chemotherapy, and cancer stem cell activity [2, 10]. Moreover, FSH has been shown to elevate Notch1 expression by the hormone in SKOV-3 cells [33]. This study demonstrates a clear association between FSH and Notch in the context of ovarian cancer metastasis. Evidence for active FSH signaling in three distinct ovarian cancer cell lines has been demonstrated. All three cell lines express FSHR with affinities in the physiological range, with the OVCAR-3 cell line showing the highest FSHR density and response to the hormone. The presence of FSHR in cell lines was also confirmed by specific binding of FSHR extracellular domain a/s, which inhibited hormone binding [15], and a response indicating the antagonistic nature of this a/s.

FSH increased overall Notch signaling by upregulation of different Notch receptors, ligands, and the downstream target genes, and in the presence of both FSH and Dll4 there was an additive increase in the Notch signaling. Increased proliferation of the ovarian cancer cell lines by FSH, as demonstrated in previous reports [6, 34], was mediated by increased Notch signaling because it was inhibited by Notch3 NRR-specific ScFv. The proliferation was brought below basal rates by the combination of Notch3 NRR ScFv and FSHR a/s.

Progression of ovarian cancer often leads to accumulation of ascites in the peritoneal cavity, which provides a complex mixture of soluble factors and cellular components,
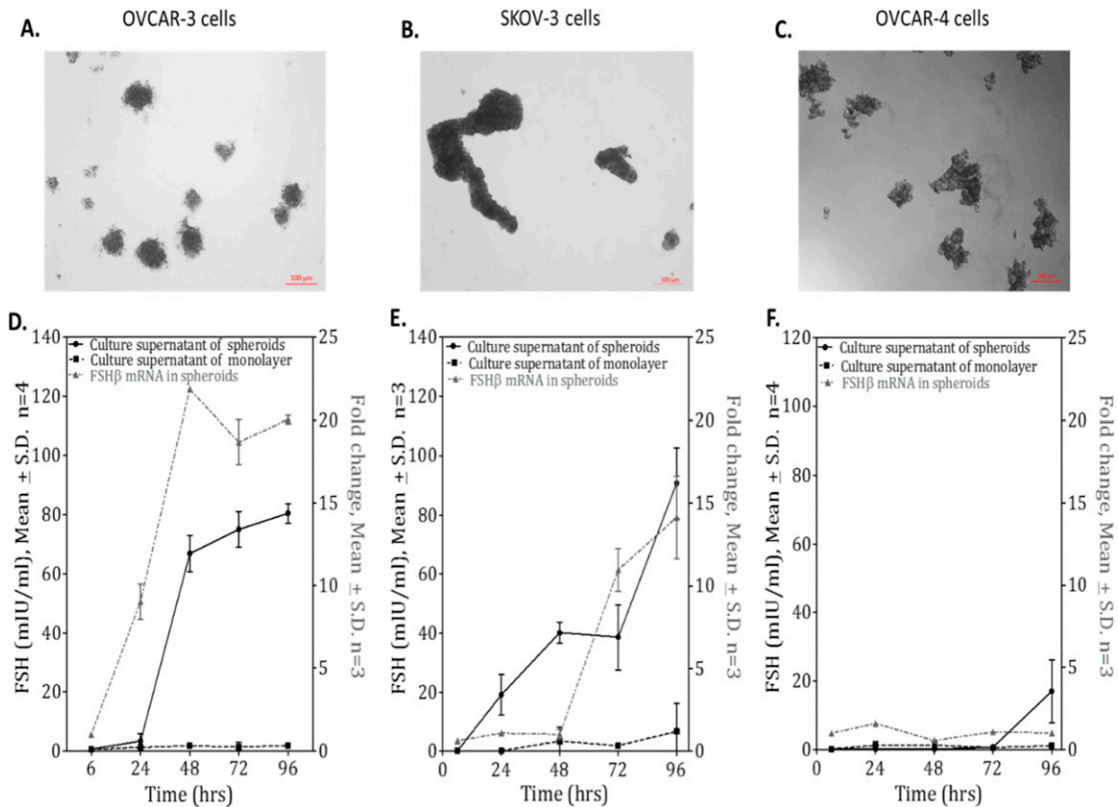
Figure 9. Expression of FSH in ovarian cancer cell line spheroids. Photomicrographic images of cellular aggregates of (A) OVCAR-3, (B) SKOV-3, and (C) OVCAR-4 cells cultured in low-attachment conditions. (D) OVCAR-3, (E) SKOV-3, and (F) OVCAR-4 cultured in low-attachment conditions or as monolayers. FSH levels in the conditioned media of aggregates/spheroids or monolayers cultured for different time periods were analyzed by RIA. RT-PCR was performed to assay the transcript levels of *FSHβ* in cellular aggregates. Fold change was calculated with respect to cells cultured as monolayers after normalizing with *GAPDH* expression. Significance was calculated by comparison of treated and basal values *via* nonparametric unpaired *t* test. n is the number of repeats. Error bars represent mean ± SD.

creating a proinflammatory and tumor-promoting microenvironment for the cells [35]. FSH is probably one such factor, and its levels in the ascites of 12 patients out of 26 patients with ovarian cancer were significantly high. Earlier reports [36] also indicated the serum/tumor fluid FSH ratios to be low in patients with ovarian cancer, suggesting that the origin of FSH in the ascites may not be the serum, which could be higher given the postmenopausal status of many of the patients [37]. However, the current study posits that spheroids obtained from the ascites are the source of FSH. We observed that OVCAR-3 and SKOV-3 cells expressed *FSHβ* mRNA and secreted FSH into the medium only when cultured as spheroids, not when grown as monolayers. Expression of the *α* subunit mRNA was observed in the cancer cell lines cultured both as monolayers and as spheroids, as well as the spheroids obtained from the patients. In contrast, *FSHβ* expression is seen only when cells are organized in spheroidal geometries. In support of our cell line–based studies, the expression of *FSHβ* (and even FSHα) was observed to be very low in cells from the primary ovarian patient tumor samples. Despite low ligand expression, FSHR expression was high. This suggests that FSH secreted by the ascitic spheroids might not just affect the morphogenesis of the latter but also turn on FSH signaling in the FSHR-expressing primary tumor driving its proliferation. However, this feedback loop depends on establishment of the metastatic niche and might be one of the earliest examples of how the metastatic niche feeds back to alter the behavior of the primary tumor niche of a cancer. Moreover, high levels of FSH in the ascites of patients with ovarian cancer are inversely correlated to their survival [37].
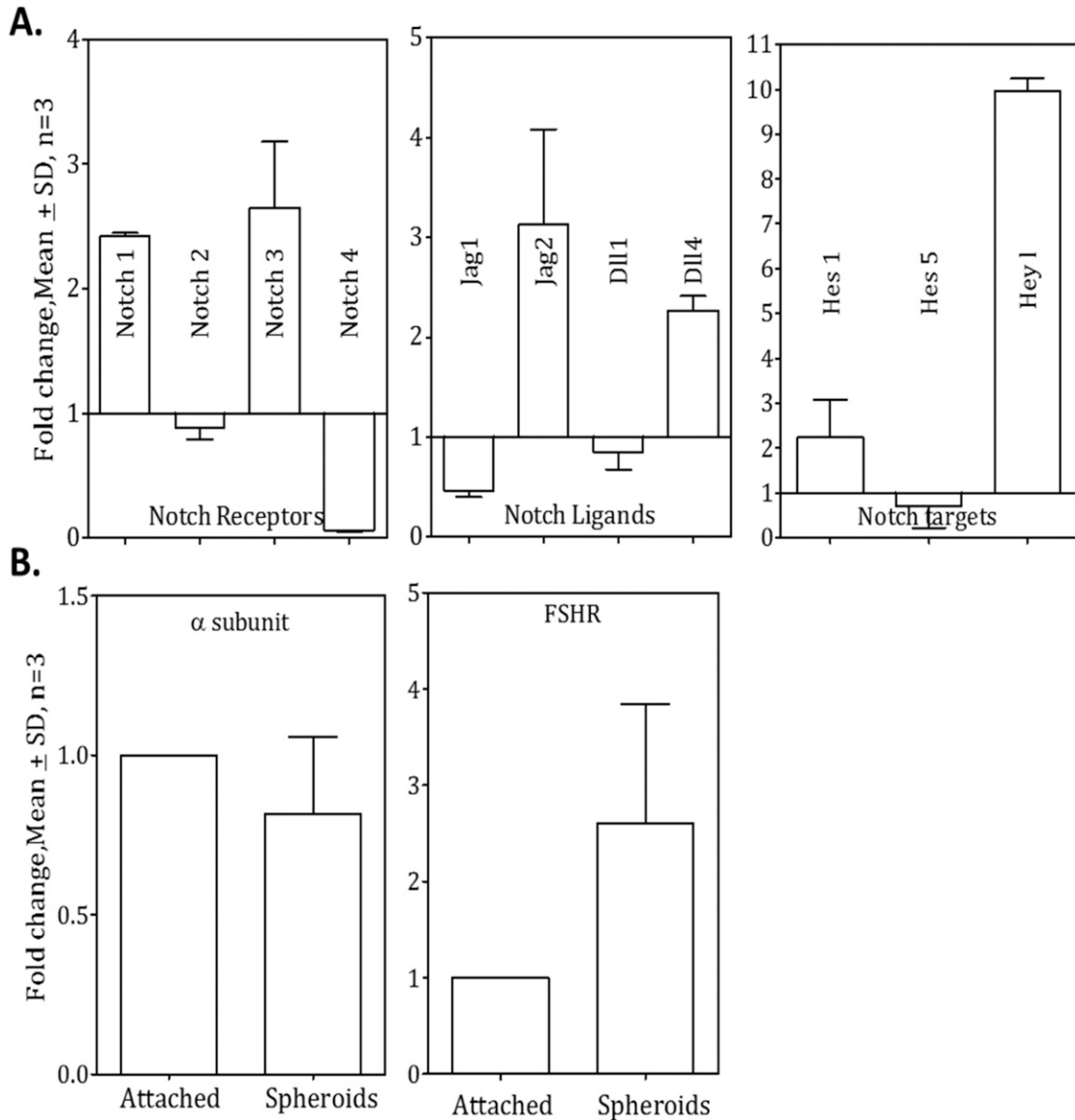
Figure 10. Status of Notch and FSH signaling genes in OVCAR-3 spheroids. OVCAR-3 cells were cultured in low-attachment conditions or as monolayers and harvested after 48 h. RT-PCR was performed to assay the transcript levels of indicated (A) Notch receptors, ligands, targets, and (B) FSHR and FSHα subunit. The fold change in the expression level of genes was calculated with respect to OVCAR-3 cells cultured as monolayers after normalizing with GAPDH expression. Error bars represent mean ± SD, and n is the number of repeats.

It is well established that FSHβ expression is the rate-limiting step in secretion of pituitary hormone [38], and once the β subunit expression is turned on, the heterodimeric hormone is secreted into the environment. The prospect of turning on FSHβ expression in the spheroids is intriguing. Spheroids have been known to show altered epigenetic regulation with a general increase in histone acetylation [39]. However, the effect on FSHβ expression appears to be specific because the expression of LHβ is not upregulated, nor was there any LH secretion under these conditions. Therefore, whether such a spheroid-specific expression and secretion of FSH indicates a metastatic, niche-specific secretome must be investigated further.

It is evident that FSH expressed by ovarian cancer spheroids upregulates Notch signaling, which together with stromal Dll4 leads to increased proliferation of tumor cells. Spheroidal cells also exhibited higher expression of FSHR, probably making them extremely sensitive to
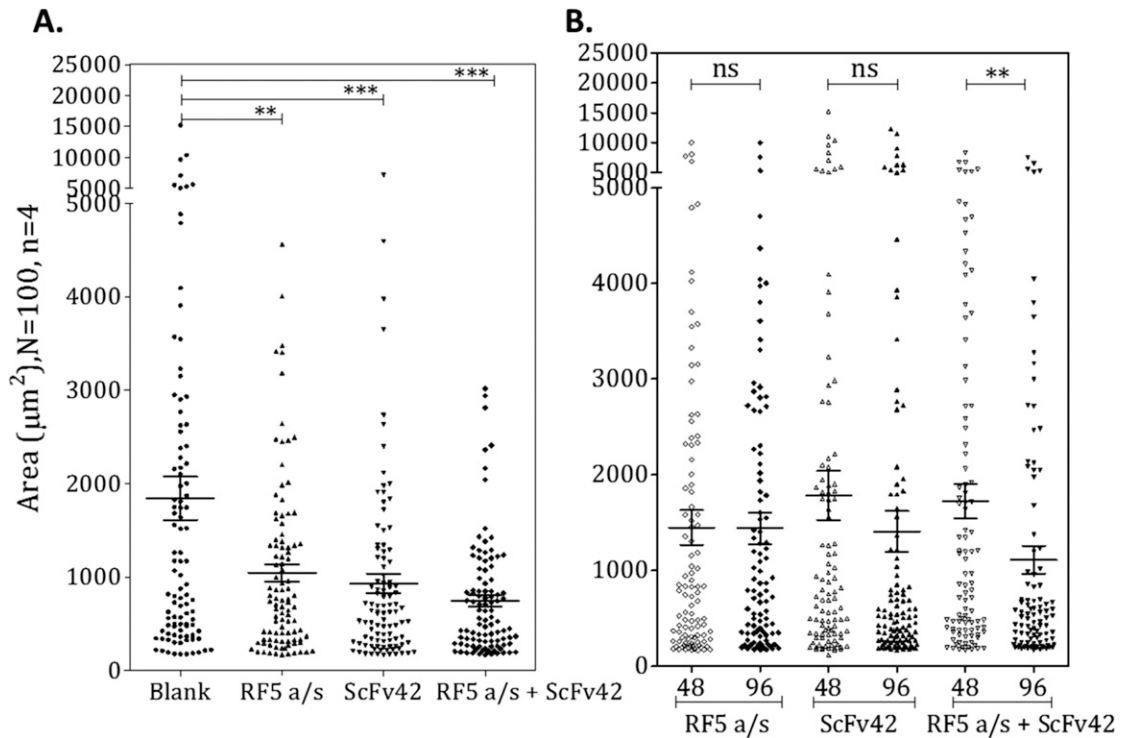
Figure 11. Effects of FSH and Notch antagonist (RF5 a/s and ScFv42, respectively) on the aggregation of OVCAR-3 spheroids. (A) OVCAR-3 cells were cultured in low-attachment conditions in the presence of RF5 a/s (5 µg/mL) and ScFv42 (10 µg/mL) individually and in combination for 48 h, and images were taken (5 fields per well) before and after the treatment. The area of the spheroids in each image was analyzed in MATLAB. The distribution of area of the 100 OVCAR-3 spheroids cultured in the presence and absence of antagonists is plotted. Each symbol represents the area of a single spheroid. (B) OVCAR-3 spheroids cultured for 48 h were incubated with RF5 a/s (5 µg/mL), ScFv42 (10 µg/mL), or both, and the microscopic images were taken at regular intervals as above. The area of the spheroids in each image was analyzed in MATLAB. Distribution of area of the 100 spheroids was measured at 48 h (before the addition of antagonists) and at 96 h (*i.e.,* 2 d after addition). Each symbol represents one spheroid, and the solid symbols represent the spheroids incubated with different antagonists. Significance was calculated by comparison of treated and basal values *via* ANOVA. Error bars represent mean ± SEM, n represents the number of repeats, and N is the number of spheroids analyzed. ns, $P > 0.05$; *$P \leq 0.05$; **$P \leq 0.01$; ***$P \leq 0.001$ compared with nontreated.

increasing concentrations of the hormone. These data indicate that there is an autocrine regulation of FSH-FSHR signaling that plays an important role in ovarian cancer progression.

Ovarian cancer cell spheroids are known to be strongly associated with the recurrence of ovarian cancer, because they show resistance to chemotherapies and radiotherapies, with larger spheroids being more resistant to the therapies [13]. Under these conditions, both FSH and Notch pathways are interesting immunotherapeutic targets. Notch NRR ScFv42, individually and in combination with the FSHR a/s, significantly inhibited formation of bigger OVCAR-3 spheroids. The antibodies also decreased the average size of the preformed spheroids. These two antibodies also inhibited ovarian cancer cell proliferation, further suggesting the therapeutic potential of these antibodies. Our observation that the FSHR antibody can perturb spheroidal morphogenesis individually but inhibit proliferation of monolayers only in an FSH-added condition suggests a morphology-specific higher activity of FSH signaling and its integration with the Notch signal transduction. The mechanistic investigations of such signaling crosstalk will be explored in future endeavors.

In conclusion, this study establishes a clear link between FSH and Notch in ovarian cancer progression and shows that these are potential targets for future therapeutic efforts.

Acknowledgments

References and Notes

1. Jemal A, Bray F, Center MM, Ferlay J, Ward E, Forman D. Global cancer statistics. *CA Cancer J Clin*. 2011;**61**(2):69–90.
2. Choi J-H, Wong AS, Huang H-F, Leung PC. Gonadotropins and ovarian cancer. *Endocr Rev*. 2007;**28**(4): 440–461.
3. Gwinn ML, Lee NC, Rhodes PH, Layde PM, Rubin GL. Pregnancy, breast feeding, and oral contraceptives and the risk of epithelial ovarian cancer. *J Clin Epidemiol*. 1990;**43**(6):559–568.
4. Havrilesky LJ, Moorman PG, Lowery WJ, Gierisch JM, Coeytaux RR, Urrutia RP, Dinan M, McBroom AJ, Hasselblad V, Sanders GD, Myers ER. Oral contraceptive pills as primary prevention for ovarian cancer: a systematic review and meta-analysis. *Obstet Gynecol*. 2013;**122**(1):139–147.
5. Ryle M. Gonadotropins and ovarian function. *Acta Eur Fertil*. 1973;**4**(3):113–122.
6. Zheng W, Lu JJ, Luo F, Zheng Y, Feng Y, Felix JC, Lauchlan SC, Pike MC. Ovarian epithelial tumor growth promotion by follicle-stimulating hormone and inhibition of the effect by luteinizing hormone. *Gynecol Oncol*. 2000;**76**(1):80–88.
7. Syed V, Ulinski G, Mok SC, Ho S-M. Reproductive hormone-induced, STAT3-mediated interleukin 6 action in normal and malignant human ovarian surface epithelial cells. *J Natl Cancer Inst*. 2002;**94**(8): 617–629.
8. Zhang Z, Zhu Y, Lai Y, Wu X, Feng Z, Yu Y, Bast RC Jr, Wan X, Xi X, Feng Y. Follicle-stimulating hormone inhibits apoptosis in ovarian cancer cells by regulating the OCT4 stem cell signaling pathway. *Int J Oncol*. 2013;**43**(4):1194–1204.
9. Huang Y, Jin H, Liu Y, Zhou J, Ding J, Cheng KW, Yu Y, Feng Y. FSH inhibits ovarian cancer cell apoptosis by up-regulating survivin and down-regulating PDCD6 and DR5. *Endocr Relat Cancer*. 2010; **18**(1):13–26.
10. Rose SL. Notch signaling pathway in ovarian cancer. *Int J Gynecol Cancer*. 2009;**19**(4):564–566.
11. Shield K, Ackland ML, Ahmed N, Rice GE. Multicellular spheroids in ovarian cancer metastases: biology and pathology. *Gynecol Oncol*. 2009;**113**(1):143–148.
12. Green SK, Francia G, Isidoro C, Kerbel RS. Antiadhesive antibodies targeting E-cadherin sensitize multicellular tumor spheroids to chemotherapy in vitro. *Mol Cancer Ther*. 2004;**3**(2):149–159.
13. Gong X, Lin C, Cheng J, Su J, Zhao H, Liu T, Wen X, Zhao P. Generation of multicellular tumor spheroids with microwell-based agarose scaffolds for drug testing. *PLoS One*. 2015;**10**(6):e0130348.
14. RRID:AB_2755044.
15. Agrawal G, Dighe RR. Critical involvement of the hinge region of the follicle-stimulating hormone receptor in the activation of the receptor. *J Biol Chem*. 2009;**284**(5):2636–2647.
16. RRID:AB_2750945.
17. RRID:AB_2750944.

18. Gera S, Dighe RR. The soluble ligand Y box-1 activates Notch3 receptor by binding to epidermal growth factor like repeats 20-23. *Arch Biochem Biophys*. 2018;**660**:129–36.

19. Dighe RR, Moudgal NR. Use of α- and β-subunit specific antibodies in studying interaction of hCG with Leydig cell receptors. *Arch Biochem Biophys*. 1983;**225**(2):490–499.

20. Chao G, Lau WL, Hackel BJ, Sazinsky SL, Lippow SM, Wittrup KD. Isolating and engineering human antibodies using yeast surface display. *Nat Protoc*. 2006;**1**(2):755–768.

21. RRID:AB_2752226.

22. Fraker PJ, Speck JC Jr. Protein and cell membrane iodinations with a sparingly soluble chloroamide, 1,3,4,6-tetrachloro-3a,6a-diphrenylglycoluril. *Biochem Biophys Res Commun*. 1978;**80**(4):849–857.

23. Kene PS, Dighe RR, Mahale SD. Delineation of regions in the extracellular domain of follicle-stimulating hormone receptor involved in hormone binding and signal transduction. *Am J Reprod Immunol*. 2005;**54**(1):38–48.

24. Sharma A, Rangarajan A, Dighe RR. Antibodies against the extracellular domain of human Notch1 receptor reveal the critical role of epidermal-growth-factor-like repeats 25–26 in ligand binding and receptor activation. *Biochem J*. 2013;**449**(2):519–530.

25. Sharma A, Paranjape AN, Rangarajan A, Dighe RR. A monoclonal antibody against human Notch1 ligand binding domain depletes subpopulation of breast cancer stem-like cells. *Mol Cancer Ther*. 2012;**11**(1):77–86.

26. Kuhnert F, Chen G, Coetzee S, Thambi N, Hickey C, Shan J, Kovalenko P, Noguera-Troise I, Smith E, Fairhurst J, Andreev J, Kirshner JR, Papadopoulos N, Thurston G. Dll4 blockade in stromal cells mediates antitumor effects in preclinical models of ovarian cancer. *Cancer Res*. 2015;**75**(19):4086–4096.

27. Desai MP, Bhanuprakash KV, Khatkhatay MI, Donde UM. Age-related changes in bone turnover markers and ovarian hormones in premenopausal and postmenopausal Indian women. *J Clin Lab Anal*. 2007;**21**(2):55–60.

28. Prasad B, Parmar D, Sharma NC. A study on serum FSH, LH and prolactin levels among infertile women. *Int J Med Res Health Sci*. 2015;**4**(4):876–878.

29. Sodek KL, Ringuette MJ, Brown TJ. Compact spheroid formation by ovarian cancer cells is associated with contractile behavior and an invasive phenotype. *Int J Cancer*. 2009;**124**(9):2060–2070.

30. Ip CKM, Li S-S, Tang MYH, Sy SKH, Ren Y, Shum HC, Wong AST. Stemness and chemoresistance in epithelial ovarian carcinoma cells under shear stress. *Sci Rep*. 2016;**6**:26788.

31. Rahman MT, Nakayama K, Rahman M, Katagiri H, Katagiri A, Ishibashi T, Ishikawa M, Iida K, Nakayama S, Otsuki Y, Miyazaki K. Notch3 overexpression as potential therapeutic target in advanced stage chemoresistant ovarian cancer. *Am J Clin Pathol*. 2012;**138**(4):535–544.

32. Vathipadiekal V, Saxena D, Mok SC, Hauschka PV, Ozbun L, Birrer MJ. Identification of a potential ovarian cancer stem cell gene expression profile from advanced stage papillary serous ovarian cancer. *PLoS One*. 2012;**7**(1):e29079.

33. Park Y-H, Kim SJ, Jeong B-H, Herzog TJ, Wright J, Kitajewski J, Rhim CC, Jang PR, Kang JB, Kim SJ. Follicular stimulating hormone enhances Notch 1 expression in SK-OV-3 ovarian cancer cells. *J Gynecol Oncol*. 2010;**21**(2):119–124.

34. Sicinski P, Donaher JL, Geng Y, Parker SB, Gardner H, Park MY, Robker RL, Richards JS, McGinnis LK, Biggers JD, Eppig JJ, Bronson RT, Elledge SJ, Weinberg RA. Cyclin D2 is an FSH-responsive gene involved in gonadal cell proliferation and oncogenesis. *Nature*. 1996;**384**(6608):470–474.

35. Ahmed N, Stenvers KL. Getting to know ovarian cancer ascites: opportunities for targeted therapy-based translational research. *Front Oncol*. 2013;**3**:256.

36. Rzepka-Górska I, Chudecka-Głaz A, Kosmowska B. FSH and LH serum/tumor fluid ratios and malignant tumors of the ovary. *Endocr Relat Cancer*. 2004;**11**(2):315–321.

37. Chen FC-K, Oskay-Ozcelik G, Bühling KJ, Köpstein U, Mentze M, Lichtenegger W, Sehouli J. Prognostic value of serum and ascites levels of estradiol, FSH, LH and prolactin in ovarian cancer. *Anticancer Res*. 2009;**29**(5):1575–1578.

38. Burger LL, Haisenleder DJ, Dalkin AC, Marshall JC. Regulation of gonadotropin subunit gene transcription. *J Mol Endocrinol*. 2004;**33**(3):559–584.

39. Paullin T, Powell C, Menzie C, Hill R, Cheng F, Martyniuk CJ, Westerheide SD. Spheroid growth in ovarian cancer alters transcriptome responses for stress pathways and epigenetic responses. *PLoS One*. 2017;**12**(8):e0182930.